Proceedings of ISFOG 2025
5TH INTERNATIONAL SYMPOSIUM ON
FRONTIERS IN OFFSHORE GEOTECHNICS
Nantes, France | June 9-13 2025

ISBN 978-2-85782-758-0

Finite element analysis of a shared pile anchor in sand under inclined multidirectional cyclic loading

X. Dias
University of Southampton, Southampton, UK

B. Cerfontaine*, K. Wen
University of Southampton, Southampton, UK

**b.cerfontaine@soton.ac.uk*

ABSTRACT: Mooring several floating offshore wind turbines to a shared anchor is a strategy to reduce the number of anchors by up to 60%, hence lowering the capital expenditure and minimising the disturbance to marine ecosystems. However, this approach introduces complex multidirectional cyclic loading onto the anchor and a more vertically inclined net force, posing risks of ratcheting failure and degradation of the axial resistance, hence of premature failure. This paper employs 3D finite-element analysis to investigate the cyclic behaviour of a multi-line pile anchor in sand with a semi-taut mooring. The SANISAND-MS constitutive model was used to simulate the nonlinear cyclic behaviour of drained sands. Initially, the model is validated against centrifuge tests conducted on piles in dense sand. The responses of the pile to four cyclic load patterns at cyclic magnitudes ranging from 20 – 50% of the pile monotonic ultimate capacity are compared: one-way, two-way and two multidirectional load patterns with varying angular variations in the horizontal plane. The findings indicate cyclic load patterns with larger angular variations in plane are more detrimental in terms of vertical ratcheting and axial shaft resistance degradation of the pile. Larger angular variation induces stress paths with larger amplitude and a greater induced displacement around the pile, hence a reduction on average of the average normal effective stress acting on the shaft, hence its capacity. Those results show that the effect of storms acting in multiple direction over the lifetime of the turbine can be more detrimental than the slight change in net force variation during a single storm event.

Keywords: Anchors; Shared anchors; Floating Offshore Wind; Cyclic loading

1 INTRODUCTION

In the UK alone, it is expected that up to 3400 – 4500 anchors will need to be installed every year by 2050 (Cerfontaine, et al., 2023) to keep floating wind turbines in place and to meet net zero objectives. These numbers exceed the capacity of the supply chain and jeopardize the achievements of carbon neutrality.

Shared anchors (or multiline anchors) are a new technology that consists of attaching several mooring lines to a single anchor. So far, they have only been implemented in one operational floating offshore wind project named 'Hywind Tampen' (Equinor, 2023). They have the advantages of reducing the number of anchors to be installed by up to 2/3, and also reducing the peak in-plane load applied to the anchor during a storm, as all mooring lines are pulling in opposite directions (Pillai, et al., 2022; Fontana, et al., 2018).

However, shared anchors are also subjected to a more complex cyclic loading over their lifetime. First, while the horizontal component of the load applied to the anchors is reduced (mooring lines pulling in opposite directions), their vertical components add up, which results in a more vertical net force. This is particularly true in (semi-)taut configurations, which can be used to reduce the footprint of mooring systems. Second, the net force acting on the pile will often be aligned with the main direction of a storm acting on the floating wind turbines. While this direction is broadly constant during the duration of a single storm, it can change from storm to storm. Therefore, the shared anchor will be subjected to a net force whose direction in plane will vary during each storm (Fontana, et al., 2018; Pillai, et al., 2022).

Those two loading cases, combining a change of direction with cyclic horizontal and vertical loading, may induce a greater risk of anchor vertical ratcheting and premature failure. To date, it is still unclear which load patterns are the most detrimental for shared anchors. This paper will undertake finite element simulations to investigate the cyclic behaviour of a shared pile anchor in a taut mooring configuration. Several tensile load patterns will be considered including one-way, two-way, and multi-directional cyclic loading (out of plane loading) which will all be undertaken at a load inclination of 30° to the horizontal. These will be tested at a variety of cyclic load magnitudes, ranging from 20% to 50% of the pile ultimate monotonic capacity.

2 FINITE ELEMENT MODEL

A 3D numerical model of a pile shared anchor was simulated in the finite element software PLAXIS3D (Bentley, 2023) and subjected to 4 simplified load patterns of varying amplitudes.

2.1 Geometry

The soil domain was modelled as a 40m x 40m x 30m (depth) cube and discretised by 12419 tetrahedral elements. The pile is 2.2m in diameter (D) and 15.5m in length (L), and was simulated using shell elements, wished-in-place in the soil volume elements. The closest distance of the pile to the boundary is equal to 9D, which is lower than 15D recommended by a previous study (Dong, et al., 2017). However, this relatively smaller domain was used to reduce computation time. It was verified that the stress field modifications induced by the pile into the soil domain does not extend to the boundary.

2.2 Constitutive model

The SANISAND-MS model available in PLAXIS 3D was chosen to predict the high-cyclic ratcheting of drained sands (Liu, et al., 2019). The model framework is based on the SANISAND04 model while introducing the concept of Memory Surface (MS) to track the loading history and to account for the fabric effects on cyclic ratcheting response of sands. Its capability to predict the tilting response of monopiles under a high number of cycles has been recently demonstrated by (Liu, et al., 2022).

The calibration of the model parameters was out of the scope of this study. Therefore, the basic set of SANISAND parameters, corresponding to the UWA silica sand calibrated by Roy et al. (2021) was used, while the parameters pertaining to memory surfaces were referred to (Liu, et al., 2022). The soil was considered homogeneous, at a 75% relative density. The loading was assumed drained, which is a reasonable assumption for piles of these dimensions in permeable sands.

The pile-soil interface was modelled by zero-thickness elements, with normal and shear elastic stiffness set to be kn = 1GPa and ks = 100MPa respectively. The penalty approach was used to simulate interface properties, and the interface friction angle (=21°) was selected as two third of the critical state friction angle in the soil (=31.5°). A nominal cohesion of 3 kPa was adopted for interface to ensure the numerical convergence of the model.

The behaviour of the pile was considered elastic linear and steel properties were assigned to the pile (E = 210GPa, ν = 0.3). The top of the anchor was assigned a higher stiffness to apply efficiently a concentrated load at its centre.

2.3 Simulations undertaken

A total of 21 simulations was undertaken to validate the numerical model and explore how multidirectional loading affects the anchor performance.

2.3.1 Validation of the model: monotonic loading

The model was first validated by comparison against centrifuge experiments undertaken by (Huang, et al., 2020), whose geometry is described in section 2.1. The pile was monotonically loaded by prescribing a displacement, applied at the centre of the top surface of the pile, along five load inclinations $\theta = [0^o\ 30^o\ 45^o\ 60^o\ 90^o]$ (relative to the seabed). Failure was defined when the net displacement of the pile head centre reached 0.1D.

2.3.2 Cyclic loading patterns

Embedded padeyes enhance a pile anchor lateral resistance, but also pose the risk of excessive vertical loading when the mooring chain is vertical, just after installation. Therefore, it was assumed that the padeye of the shared pile was located at the centre of its head.

Shared anchors load paths can be particularly complex and varied (Herdiun, 2019) when all mooring lines are considered independently. Therefore, it was decided to simulate only the net force load path, which results from the simultaneous application of three mooring forces. The angle of this net force to the horizontal was kept constant at 30°. This actually corresponds to mooring lines inclined at a lower angle to the horizontal in a semi-taut mooring system.

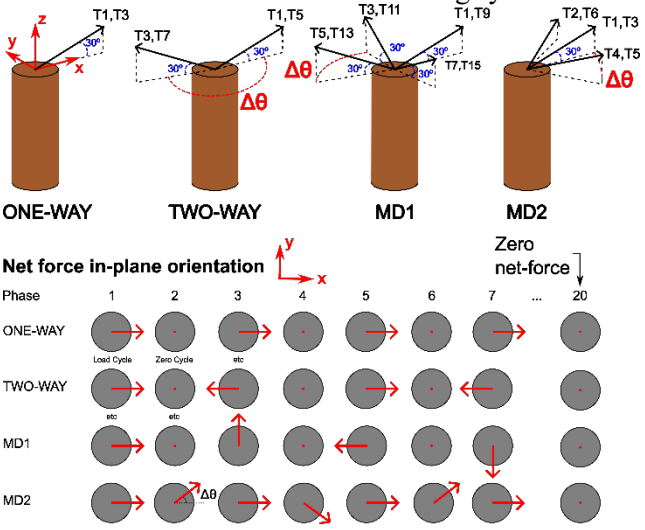

Figure 1 Definition of the four cyclic loading patterns. MD1 and MD2 = multidirectional. $\Delta\theta$ is the angular variation of the net force in plane.

Four distinct cyclic load patterns were investigated in this work (Figure 1): one-way, two-way, and two variations of multidirectional loading, denoted as MD1 and MD2. In all cases, the load was assumed to be quasi-static.

The one-way pattern is taken as a reference non-shared anchor subjected to a single storm event. It is always loaded in the same direction. The choice of multidirectional load patterns relies on the assumption that the net force applied to the shared anchor tends to be aligned with the main direction of any given storm (Fontana, et al., 2018), though the angle in plane can vary slightly. Therefore, there are two main sources of multidirectionality. At the scale of a single storm, the orientation of the net force in plane varies around the main direction of the storm (MD2 case). At the scale of the turbine lifetime, the net force orientation in plane aligns to the main direction of each successive storm, which we assume rotate by 90° each cycle as an extreme case (MD1). The two-way pattern considers a variation of 180° between two storms, while the MD2 pattern considers successive variations of an angle $\Delta\theta$.

The magnitude of the cyclic load is given as a percentage of the ultimate monotonic capacity of the pile at a 30° inclination ($F_{ult,30}$), defined by the non-dimensional parameter proposed by (Leblanc, et al., 2010).

$$\zeta_b = \frac{F_{max}}{F_{ult,30}}$$

The ultimate capacity, $F_{ult,30}$ is the load at which the net pile head displacement reached 0.1D (220 mm), as no plateau could be achieved for a "small" displacement. In all load patterns but MD2, the cyclic loads alternate between the maximum value and zero. In the MD2 case, the load magnitude remains constant, but its direction varies, before being reduced to 0.

Ten cycles were completed in all configurations to limit the necessary computational time. Following the completion of the last cycle in each configuration, a subsequent vertical and horizontal monotonic test was conducted to assess the post-cyclic capacity of the pile.

3 RESULTS

3.1 Validation

Figure 2 compares the failure envelopes between the experimental (centrifuge) results (Huang, et al., 2020) and numerical simulations. In each case, the lateral (F_x) and vertical (F_z) force at failure for each inclined loading are normalised by the purely lateral and vertical resistances of the pile ($F_{x,ult}$ and $F_{z,ult}$). Note that the ultimate resistances in two cases were defined in different way. For the numerical results, failure is defined for a displacement equal to 0.1D. For centrifuge results, failure is defined by the achievement of a plateau in the measured force, which requires a much larger displacement (up to 2D for lateral loading) to be fully mobilised.

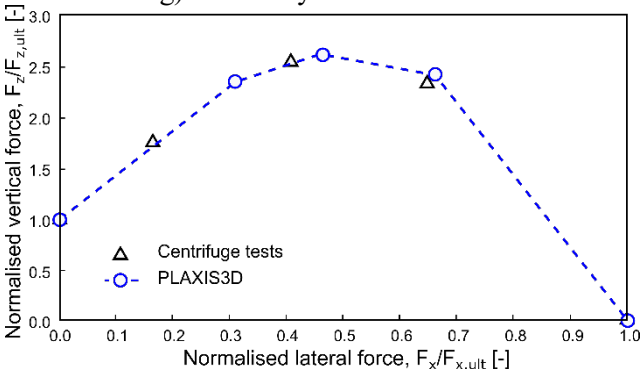

Figure 2 Comparison of the failure envelope between the experimental centrifuge and numerical results.

Despite those differences, the failure envelope obtained from experimental and numerical results are similar, and depicts an enhanced pile resistance for inclined loading, due to the positive interaction between the lateral and vertical loads. This was expected as the lateral load increases the normal stress acting on the shaft, hence the shear resistance that can be mobilised axially.

The failure load for an imposed displacement inclined at 30°, $F_{ult,30}$, is measured to be 7134 kN. The horizontal and vertical force components are equal to F_x = 5805 kN and F_z = 4147 kN, which gives a load inclination of $\theta = 35.5^o$. This discrepancy comes from the different pile kinematics induced by imposed force or displacement. However, for the purpose of this study, 7134 kN will be considered the ultimate monotonic resistance for a load imposed at 30° and used in the cyclic tests.

3.2 Displacement Response

Typical load-displacement relationships for the two-way and MD2 ($\Delta\theta = 60°$) load patterns, both with an amplitude $\zeta_b = 0.3$, are depicted in Figure 3. The lateral displacement increases with the cyclic loading in the MD2 case, but decreases for the two-way loading. The difference in accumulated vertical displacement due to cyclic loading is even greater. It increases by 2.5mm for the MD2 case, but by 28mm for the two-way loading, and exhibits some ratcheting, on the contrary to the MD2 case, which stabilises.

Figure 4 compares the final vertical displacement achieved after 10 cycles for all load patterns, as a function of the load magnitude applied to them. Unfortunately, it was not possible to conduct two-way tests at a load amplitude higher than 30% as the model could not converge. The numerical results were also

fitted using polynomial regressions for all loading patterns. This figure clearly shows that multidirectional loading with the largest angular variations in the horizontal plane ($\Delta\theta$) lead to the largest accumulated vertical displacement. In particular, the largest displacement was recorded for the MD1 ($\zeta_b = 0.5$).

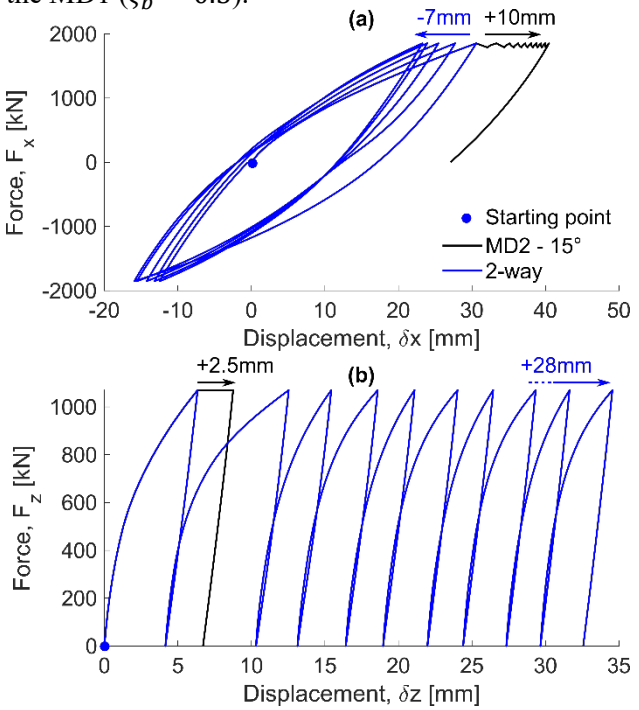

Figure 3 Comparison of typical load-displacement relationships for lateral (x-direction) and vertical (z-direction) directions, for 2-way loading ($\Delta\theta = 180°$) and MD2 with 15° amplitude ($\Delta\theta = 30°$).

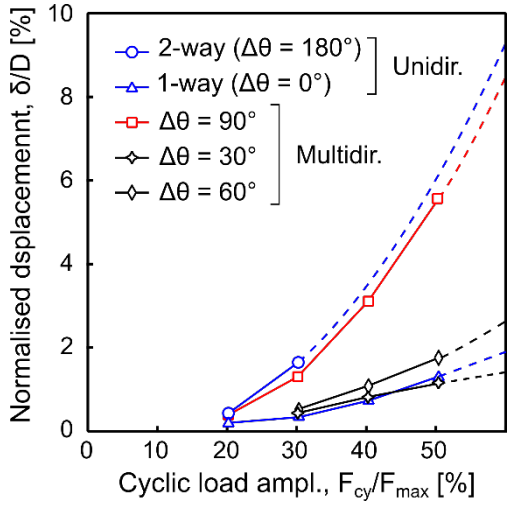

Figure 4 Comparison of the accumulated vertical displacement after 10 cycles for the different load patterns: 1-way, 2-way, MD1 ($\Delta\theta = 90°$) and MD2 ($\Delta\theta = 30°$ or $60°$). Dashed is a quadratic polynomial fit.

These findings indicate that the most detrimental case for vertical ratcheting failure mode comes from successive storms of various orientations, rather than from changes of loading direction during a single storm, although those two effects could add to each other. Therefore, preventing excessive vertical displacement may dictate the design of multi-line anchors rather than the ultimate limit state.

Results from Figure 3 can be presented as a function of the angular variation of the plane direction, as shown in Figure 4 to highlight the strong influence of this variation on the accumulated vertical displacement. Such a framework could be used to synthesise and compare results from different load patterns, otherwise difficult to compare like for like.

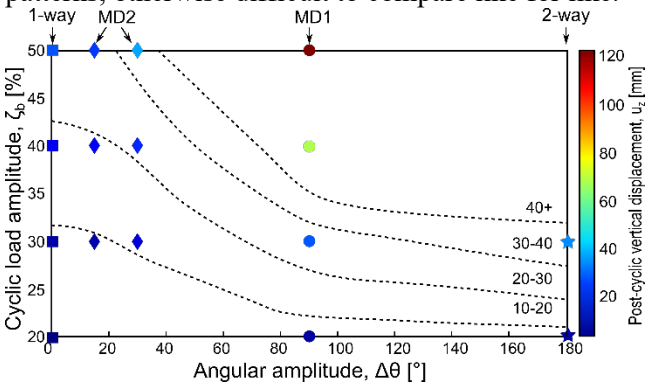

Figure 5 Vertical displacement after cyclic loading of the pile for different load patterns (1-way, 2-way, MD1, MD2)

3.3 Post-Cyclic Shaft Capacity

Post-cyclic monotonic load tests were undertaken for each of the simulated cases, to calculate its capacity, defined as the load for a pile displacement equal to 0.1D. These values were normalised by the monotonic tensile resistance before cyclic loading and are depicted in Figure 6. The results show that the shaft capacity increases with the cyclic loading of the pile, except for the two-way cyclic loading (decrease of 7%). The shaft enhancement increases with the cyclic amplitude, but is greater for the two load patterns whose average load remains in the same direction (one-way and MD2 patterns), with a maximum of up to 50% enhancement of the shaft resistance.

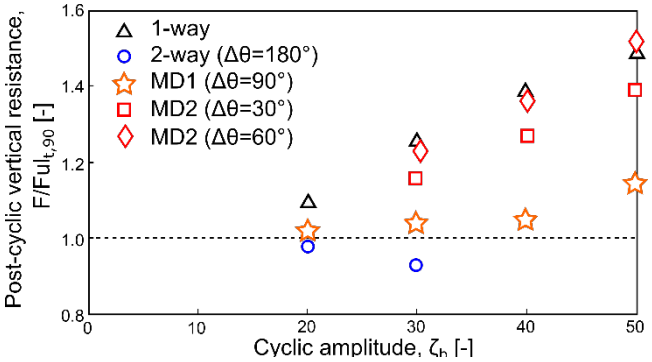

Figure 6 Normalised post-cyclic vertical monotonic resistance as a function of the cyclic load magnitude (ζ_b) and different load patterns.

All simulations exhibited a permanent vertical displacement, hence a reduction of the shaft contact area with the sand. However, this reduction was not

enough to explain a 7% reduction in resistance (2-way load pattern), and some load patterns still exhibit an increase in capacity, which needs to be explained.

3.4 Mechanisms

Figure 7a depicts the stress path of a soil element located at the front of the pile (in the x-direction), embedded 1.5m below the ground surface. The increase of the load applied to the pile logically increases the stress state in front of the pile. However, the 2-way cyclic loading seems to exhibit increasing deviatoric and average stresses with the cycle number, while the MD2 pattern shows a decreasing deviatoric stress and fairly constant average stress. Moreover, the cyclic deviatoric stress amplitude is much lower in case of the MD2 load pattern.

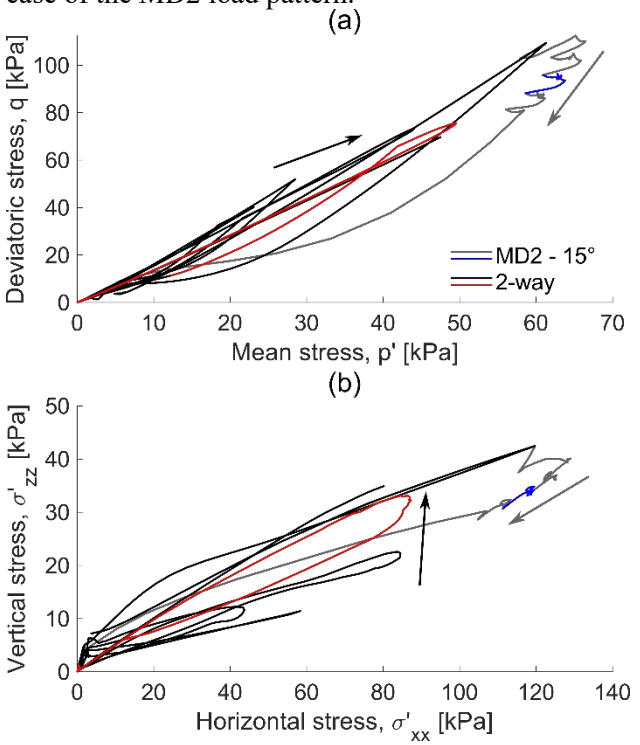

Figure 7 Stress path in an element located 0.2m from the pile front, 1.5m below the ground level. One cycle is highlighted in blue (MD2 - $\Delta\theta = 30°$) and in red (2-way)

Figure 7b shows the cartesian stress paths. The MD2 load pattern shows a higher horizontal stress (σ'_{xx}) than the two-way load pattern, and reducing vertical stress (σ'_{zz}), which is the opposite of the two-way load pattern. From those observations, it can be assumed that load patterns with greater angular variation of the net force in plane ($\Delta\theta$) will lead to a different principal stress rotation in the soil surrounding the pile. As a direct consequence, the normal stress acting on the pile shaft will increase or decrease, which will induce a reduction/enhancement in shaft resistance. The normal stress change with respect to the initial value was calculated for two cases in Figure 8, and showed the clear positive effect of the MD2 load pattern. In case of reduced shaft resistance, the axial deformation can snowball at constant load amplitude, as the cyclic load represents each time a greater proportion of the shaft resistance.

The difference in behaviour also lies in different soil deformation mechanisms at a wider scale (Figure 9). In the two-way load pattern ($\zeta_b = 0.3$), the soil at the front and back of the pile alternates between "flowing" downwards to fill a forming gap and being pushed upwards when the load reverses. On the contrary, in the MD2 case, the soil is always "flowing" downwards at the back of the pile and being pushed upwards at the front. The local (stress paths) and global (general deformation, densification/loosening) mechanisms are linked together and explain most of the macroscopic pile behaviour. However, a wider and more systematic investigation is necessary to draw more general conclusions.

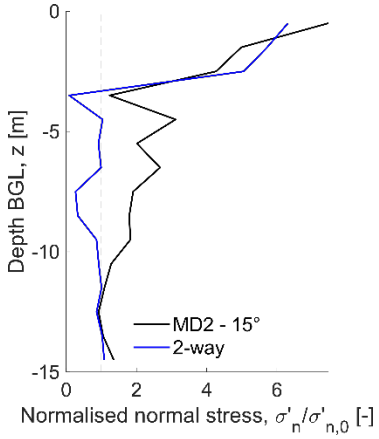

Figure 8 Profiles of average normal effective stress after cyclic loading, normalised by the initial normal effective stress, in two configurations.

4 CONCLUSIONS

The inclined loading behaviour of shared pile anchors was investigated by a 3D finite element analysis. The study comprised 16 cyclic simulations, each consisting of 10 cycles, encompassing various load patterns (one-way, two-way, and two variants of multi-directional) at load magnitudes ranging from 20-50% of monotonic ultimate capacity. All tests were conducted with a load inclination of 30° to the seabed, representing a semi-taut mooring line. The effect of load pattern and magnitude on the displacement and post-cyclic capacity was investigated.

The results show that the angular variation in plane of the direction of the net force applied to the anchor is critical to determine the shared pile behaviour. For low angular amplitudes (0 – 30°), the pile vertical displacements remained relatively low and were found to be stable over 10 cycles and the shaft capacity considerably increased after cyclic loading (up to a

51% increase). Conversely, higher angular amplitudes (90° and 180°) resulted in the highest vertical displacement and reductions in shaft capacity during two-way loading of up to 7%.

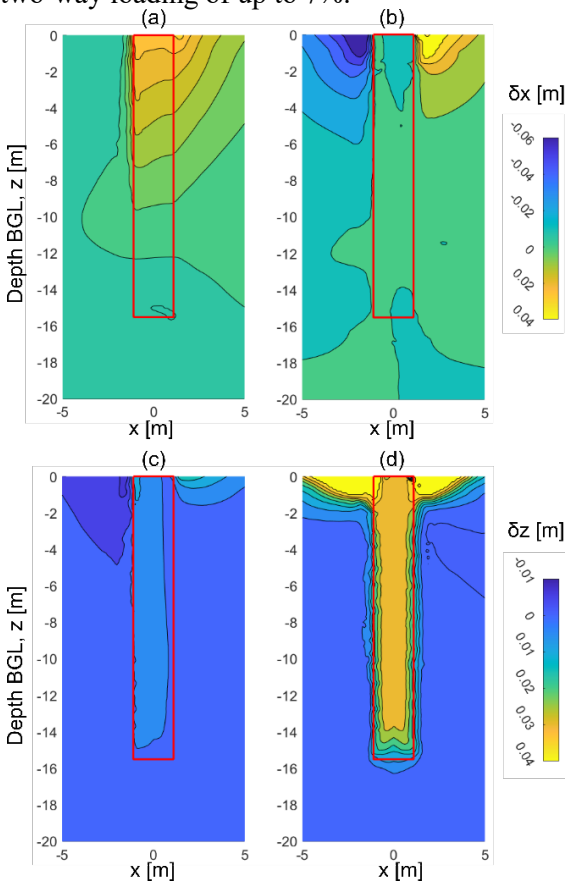

Figure 9 horizontal displacement for (a) MD2 and (b) Two-way load patterns; Vertical displacement for (c) MD2 and (d) Two-way load patterns, after cyclic loading (net force = 0). Cyclic amplitude $\zeta_b = 0.3$.

The different load patterns were linked to different deformation mechanism of the soil around the pile, and different cyclic stress paths. Greater angular change in direction of the net force resulted in less horizontal stress build up than the low angular amplitude, hence to the reduction in the shaft resistance.

This preliminary study explores the effect of the different sources of multidirectionality of the net force applied to shared anchor, which could result from slight variation of wind and wave directions during one storm, or from multiple storms of changing directions. The latter case was identified as being more detrimental for design, although much remains unknown at this stage. Future research should explore the effect of a greater number of cycles, and also of more complex load patterns.

AUTHOR CONTRIBUTION STATEMENT

X. Dias: Data curation, Formal Analysis, Writing- Original draft. **B. Cerfontaine, K. Wen**: Software, Conceptualization, Methodology, Supervision, Writing- Reviewing and Editing.

REFERENCES

Barton, Y. O., 1982. *Laterally loaded model piles in sand: centrifuge and finite element analyses..* s.l.:The University of Cambridge, PhD Thesis.

Bentley, 2023. *PLAXIS3D General Information Manual.* s.l.:s.n.

Cerfontaine, B. o.fl., 2023. Anchor geotechnics for floating offshore wind: Current technologies and future innovations. *Ocean Engineering,* Bindi 279.

Dong, J., Chen, F., Zhou, M. & Zhou, X., 2017. Numerical analysis of the boundary effect in model tests for single pile under lateral load. *Bulletrin of Engineering Geology and the Environment.*

Equinor, 2023. *Hywind Tampen.* [Á neti] Available at: https://www.equinor.com/energy/hywind-tampen

Fontana, C. o.fl., 2018. Multiline anchor force dynamics in floating offshore wind turbines. *Wind Energy (May),* 21(11), pp. 1177-1190.

Herdiun, M., 2019. *Multi-directional Loading on Shared Anchors for Offshore Renewable Energy: Definition and Preliminary Investigation into Soil Behaviour and Anchor Performance.* s.l.:s.n.

Huang, T. o.fl., 2020. Drained response of rigid piles in sand under an inclined tensile load. *Geotechnique Letters Volume 10 Issue 1,* pp. 30-37.

Leblanc, C., Houlsby, G. T. & Byrne, B. W., 2010. Response of stiff piles in sand to long-term cyclic lateral loading. *Geotechnique,* 60(2), pp. 79-90.

Lin, S.-S. & Liao, J.-C., 1999. Permanent Strains of Piles in Sand due to Cyclic Lateral Loads. *Journal of Geotechnical and Geoenvironmental Engineering,* 125(9).

Liu, H., Kementzetzidis, E., Abell, J. A. & Pisano, F., 2022. From cyclic sand ratcheting to tilt accumulation of offshore monopiles; 3D FE modelling using SANISAND-MS. *Geotechnique,* 72(9), pp. 753-768.

Liu, H. Y., Abell, J. A., Diambra, A. & Pisano, F., 2019. Modelling the cyclic ratcheting of sands through memory-enhanced bounding surface plasticity. *Geotechnique,* 69(9), pp. 783-800.

Pillai, A. o.fl., 2022. Anchor loads for shallow water mooring of a 15 MW floating wind turbine — Part I: Chain catenary moorings for single and shared anchor scenarios. *Ocean Engineering,* 266(1).